Oscillons and domain walls

Article (Published Version)

Oscillons and domain walls

Mark Hindmarsh[1,*] and Petja Salmi[1,2,+]

[1]*Department of Physics & Astronomy, University of Sussex, Brighton BN1 9QH, United Kingdom*
[2]*Lorentz Institute of Theoretical Physics, University of Leiden, P.O. Box 9506, 2300 RA Leiden, The Netherlands*

(Received 11 February 2008; published 28 May 2008)

Oscillons, extremely long-lived localized oscillations of a scalar field, are shown to be produced by evolving domain wall networks in ϕ^4 theory in two spatial dimensions. We study the oscillons in frequency space using the classical spectral function at zero momentum, and obtain that the velocity distribution is suppressed as γ^{-2} at large Lorentz factor γ, with oscillons produced up to at least $\gamma \sim 10$. This leads us to speculate that oscillons are produced at cusps, regions of the domain wall travelling near the speed of light. In order to gain some insight onto the dilute oscillon ''gas'' produced by the domain walls, we prepare a denser gas by filling the simulation volume with oscillons boosted in random directions. We finish the study by revisiting collisions between oscillons and between an oscillon and a domain wall, showing that in the latter case they can pass straight through with minimal distortion.

DOI: 10.1103/PhysRevD.77.105025 PACS numbers: 11.27.+d, 03.65.Pm, 11.10.−z

I. INTRODUCTION

There is good understanding of the formation [1–3] of coherent structures in phase transitions. While the focus has been in time-independent solutions whose stability is protected e.g. by the conservation of a topological charge, there are time-dependent solitons as well, like Q-balls and *oscillons*. The stability of Q-balls [4] is under control by charge conservation, but there is no evident guarantee for oscillons, and the longevity of these localized, nonperturbative oscillations is not well understood. They were found first already in the 1970s [5,6] and then rediscovered [7] when the dynamics of first-order phase transitions and bubble nucleation was studied (for an extended investigation, see [8]). It should be noted that oscillon is not the only term appearing in the literature for the phenomenon, but we adopt it hereafter for the rest of this study.

Oscillons have attracted quite some attention recently. A significant development has been the extension of oscillon solutions to gauge theories. The first discovery was made in gauged SU(2) model [9], where $(1 + 1)$-dimensional simulations showed that with Gaussian initial data the fields settle quickly into an oscillating state that has not been seen to decay, when the scalar and vector masses in the theory are set to be $m_H = 2m_W$. More recently, this study has been extended to SU(2) × U(1) model, describing thus the complete bosonic sector of the standard model. The full three-dimensional simulations reported in [10,11] point out that the result holds also in the presence of photons and without the assumption of spherical symmetry. Thus with the mentioned fine-tuned mass ratio there is an oscillon with energy of the order 10 TeV, yet out of reach of the current particle accelerators, but, however, much less massive than Q-balls (see e.g. [12]). The importance here does not lie merely in extending the appearance of oscillons into a wider class of theories, but also in the potential phenomenological consequences. Oscillons could, namely, provide the necessary nonequilibrium conditions needed for baryogenesis. However, one must bear in mind that an earlier investigation of the potential of thermal production of oscillons at an electroweak scale came to a negative conclusion [13].

Along the oscillon in the standard model, there are recent studies of oscillons in scalar theories [14–16]. A dedicated examination in three dimensions was carried out in [14] showing compelling evidence for a critical frequency minimizing energy and the size of the oscillon core. Similar results were communicated in [15] where, keeping the dimension of the theory a free parameter, oscillon lifetime dependence on the dimensionality was investigated (see also [17]). Most recently, compact, nonradiating, periodic solutions in $(1 + 1)$-dimensional signum-Gordon model have been reported in [16].

As solutions of nonlinear field equations, oscillons are well worth investigating, as are their effects if they are created in the early Universe. In order for oscillons to play a role, there is a need for processes to initiate large oscillations in the field in different models. The formation of oscillating energy concentrations has been reported after supersymmetric hybrid inflation [18], as well as after a tachyonic transition in an SU(2) Higgs model [19]. Similarly a study of the QCD phase transition observed dense oscillating pseudosolitons in the axion field [20] (for a study of pseudobreathers in sine-Gordon model see [21]). In [22] oscillating field configurations were reported to form with nearly quadratic potentials (as a remark, nonlinearities can also create freak waves, see e.g. [23]). Recently [24] oscillons were found as a result of vortex-antivortex annihilation in the two-dimensional Abelian-Higgs model, providing another example of oscillons in gauge theory. Once formed, oscillons could considerably

*m.b.hindmarsh@sussex.ac.uk
+salmi@lorentz.leidenuniv.nl

influence the dynamics of the system as has been suggested for the case of the bubble nucleation process [25].

While the oscillating energy concentrations have been seen to form with a tiny initial density contrast in [22], the purpose of this study is to report oscillon formation via a much more violent process, namely, from the domain collapse in ϕ^4 theory. For a related study see [26] where it has been shown that collision of two bubbles in first-order phase transition can lead to formation of long-lived quasilumps.

The paper is organized as follows. First we review the basics of the classical spectral function and examine the signal of oscillons in spectral function. We apply our method to simulations with random initial conditions, and are able to detect oscillons formed from collapsing domains, and measure their velocity distribution. In an attempt to understand the resulting ensemble of oscillons and to reduce the effect of the radiation bath they move through, we also prepare an initial state of only oscillons moving into random directions and report the dynamics of this oscillon gas. Annihilation through collision seems to play a role in reducing the density of oscillons, and so we finish our study studying the off-axis collisions of oscillons and an oscillon and a stationary domain wall.

II. NUMERICAL SETUP

The Lagrangian for a single real scalar field ϕ is given by

$$\mathcal{L} = \tfrac{1}{2}\partial_\mu\phi\partial^\mu\phi - V(\phi), \tag{1}$$

and the equation of motion thus reads

$$\ddot{\phi} - \nabla^2\phi + V'(\phi) = 0. \tag{2}$$

In this study V is the degenerate double-well quartic potential

$$V(\phi) = \tfrac{1}{4}\lambda(\phi^2 - \eta^2)^2. \tag{3}$$

The vacuum expectation value and couplings can be scaled out and set to unity. With that choice the minima are at $\phi = \pm 1$ and the local maximum at $\phi = 0$.

The field equation is evolved on a two-dimensional lattice with periodic boundary conditions using a leapfrog update and a three-point spatial Laplacian accurate to $O(dx^2)$. The lattice spacing for the data shown is set to be $dx = 0.25$ and the time step $dt = 0.05$. We utilize periodic boundary conditions throughout this study because we wish to allow oscillons to move without hitting any boundaries as well as let domains grow in simulations of random initial conditions.

III. OSCILLONS IN THE SPECTRAL FUNCTION

A. Spectral function in the classical approximation

The classical one-particle spectral function for a real scalar field ϕ can be defined through the Poisson bracket as

$$\rho(t, \boldsymbol{x}) = -\langle\{\phi(x), \phi(\mathbf{0})\}\rangle, \tag{4}$$

where the angle brackets denote an average over initial conditions. For a system in thermal equilibrium at temperature T, one can show [27,28]

$$\rho(t, \boldsymbol{x}) = -\frac{1}{T}\langle\Pi(t, \boldsymbol{x})\phi(0, \mathbf{0})\rangle, \tag{5}$$

where Π the field momentum $\dot{\phi}$.

The numerical implementation of the correlator in (5) is straightforward in leapfrog discretization. In [28] the following symmetrized definition was suggested

$$\rho(t, \boldsymbol{x}) = -\frac{1}{T}\left\langle\Pi\left(t + \frac{dt}{2}, \boldsymbol{x}\right)\frac{1}{2}(\phi(0, \mathbf{0}) + \phi(dt, \mathbf{0}))\right\rangle. \tag{6}$$

The classical spectral function at zero spatial momentum $\rho(t, \boldsymbol{p} = \mathbf{0})$ can be obtained from a volume average of (6). The spectral function in frequency space, $\rho(\omega, \mathbf{0}) \equiv \rho(\omega)$, can in turn be derived by performing Fourier transform.

We do not attempt to define temperature in what follows here, but merely adopt the correlator of the field and field momentum as a useful quantity to monitor in order to determine frequencies present in the system under the study. We simultaneously point out that our choice, inspired by the spectral function, is not unique, but other correlators, like e.g. equal time correlator of ϕ and Π, could be utilized equally well. The choice of the reference point $\boldsymbol{x} = \mathbf{0}$ of the field ϕ in (5) obviously does not play a role in a homogeneous system where no lattice site is in special position. This is not strictly true when e.g. a stationary oscillon is placed in the middle of a lattice. Instead of choosing one lattice site, simulations averaging over all points in the lattice were performed. However, even though homogeneity cannot be directly assumed, an approximation of the spectral function at zero momentum where the correlator in (5) is replaced by the product of average value of Π at given time and ϕ at reference time $t = 0$, $\rho(t) = \bar{\Pi}(t) \cdot \bar{\phi}(0)$, turns out to yield the same information in frequency space. Computationally this approximation is much more economical and will be utilized during the rest of this study.

B. Oscillon signal in the spectral function

Oscillons are created on the lattice by using a Gaussian ansatz

$$\phi(r) = (1 - C \cdot \exp(-r^2/r_0^2)), \tag{7}$$

where r is the distance to the center of an oscillon $r = (x_1^2 + x_2^2)^{1/2}$. The width of the distribution is set to be $r_0 \simeq 2.9$ [in units of $(\sqrt{\lambda}\eta)^{-1}$], suggested an optimal choice in [8] and the maximum displacement $C = 1$ so that the center of the oscillon starts from the local maximum of the potential. This choice guarantees that the field starts far

beyond the inflection point of (3) ensuring that the field probes the nonlinear features of the potential (it should be noted that much smaller amplitude has been used to initialize a scalar field e.g. in [9]). Small amplitude oscillations would be also indistinguishable from linear, dispersive fluctuations in what follows.

Oscillations take place at the basic frequency ω_0 that must be less than the threshold for radiation m, the mass in the theory. The following periodic ansatz that also assumes spherical symmetry

$$\phi(r, t) = \sum_{n=0}^{\infty} f_n(r) \cos(n\omega_0 t), \tag{8}$$

has been seen to be rapidly converging [15,29,30], thus one expects also first few integer multiples of the frequency ω_0 to appear in the spectra.

We perform a boost on an oscillon and allow it then to move on the lattice, the size of which for the data shown was set to be 400^2. During the simulation we measure the mean $\bar{\Pi}(t)$ in order to attain $\rho(t)$. Figure 1 shows the spectral function $|\rho(\omega)|$ at zero momentum obtained by performing Fourier transform over the interval of length $5 \cdot 10^3$ in time units when an oscillon is stationary and when it is moving at velocity $v \simeq 0.42$. The location of the peak of the basic frequency of a moving oscillon is shifted left to a smaller value due to time dilation and its multiples correspondingly. The effect is best visible by comparing the location of the fourth peaks in the pictures or the distance between the peak of the basic frequency and that of radiation. This drift is further illustrated in Fig. 2, where the relative frequencies where the peaks appear in the spectra are shown against inverse of the γ-factor, $\gamma = 1/\sqrt{1 - v^2}$. The deviations of measured values from the straight line $\omega = \omega_0/\gamma$ illustrate the numerical limitations of determining the basic frequency in the data as well as the precision in the velocity of a moving oscillon. The peaks at $\omega = m$ in Fig. 1 indicate the presence of a dispersive radiation component in the simulation box due to emission by an oscillon.

In addition to the shift of the basic frequency there is a much more drastic effect in the suppression of the height of the peak at the oscillation frequency as the velocity of an oscillon increases. We expect exponential decrease (see Appendix). The value of the spectral function ρ at $\omega = \omega_0(\gamma)$ is shown as a function of v^2 together with the prediction in Fig. 3. We immediately point out that the precision in measuring the amplitude is not expected to be good. This is due to the restricted resolution in the frequency (order 10^{-3} in units of ω/m) when a discrete Fourier transform in a limited interval is carried out, whereas the peak itself is generally very narrow. Furthermore, while time dilation shifts the location of the oscillation frequency further away from the radiation frequency thus easing the distinction between these two, the strength of the signal gets strongly suppressed.

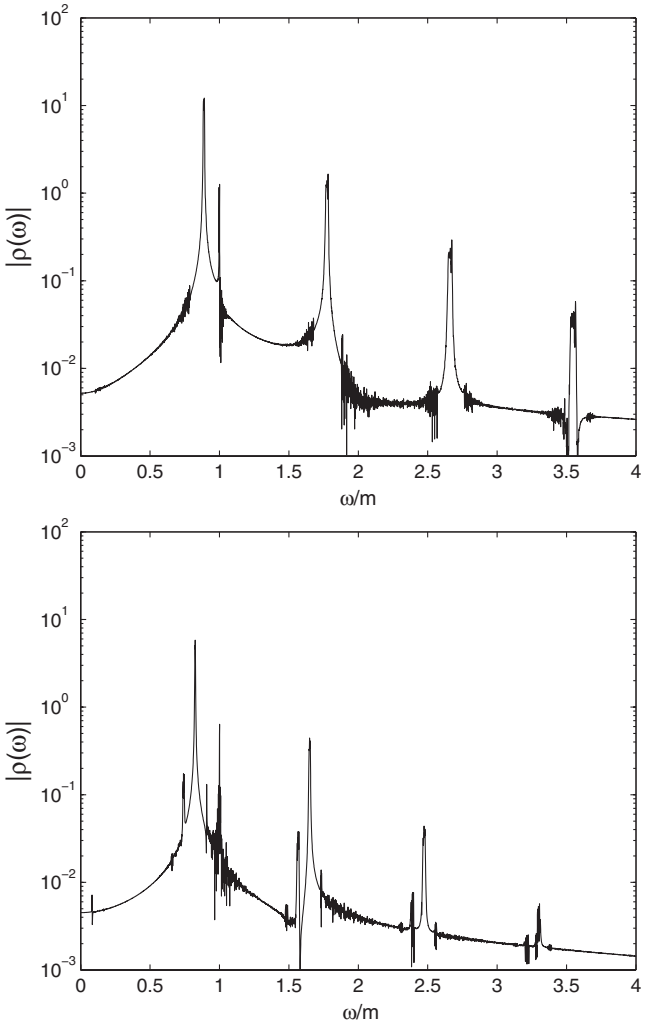

FIG. 1. The spectral function $|\rho(\omega)|$ at zero momentum over the time interval of length $5 \cdot 10^3$ for a stationary oscillon (above) and an oscillon with velocity $v \simeq 0.42$ (below).

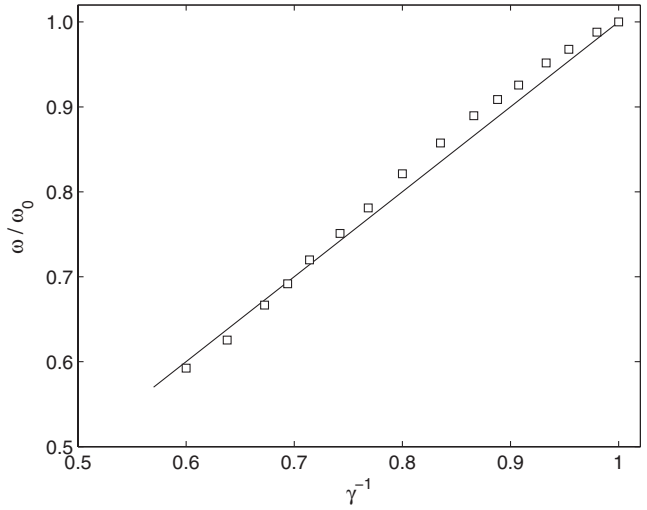

FIG. 2. The relative frequency ω/ω_0 as a function of the inverse of the γ-factor. The solid line is $\omega = \omega_0/\gamma$.

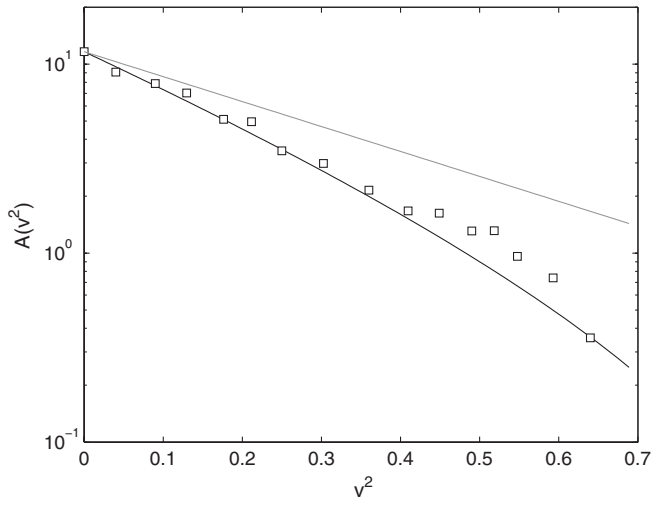

FIG. 3. The amplitude of the basic frequency, i.e. the power in the spectral function $\rho(\omega)$ at its peak, as a function of velocity. The black solid curve shows the right-hand side of the Eq. (A4) while the gray straight line demonstrates the bare exponential $\exp(-\omega_0^2 r_0^2 v^2/2)$ without the additional power suppression. The curves are fitted to have the value 11.63 at $v = 0$; $\omega_0 = 0.85$, and $r_0 = 2.9$.

Consequently, the positions of the data points in Fig. 3 can be considered only indicative.

IV. RADIATION OF OSCILLONS FROM COLLAPSING DOMAINS

We use the algorithm briefly described in the second section initialized now with random conditions. Equation (2) is evolved numerically on a lattice of size 400^2 (keeping the lattice spacing $dx = 0.25$ throughout this study, the physical size in linear dimension L is 100). We use ''false vacuum'' initial conditions; the field is set to the local maximum of the potential, and the field momentum is given a random value picked from a Gaussian distribution with a zero mean and the width 0.1. This means that the correlation length ξ at the beginning of the simulation, if not exactly zero, is less than the lattice spacing, $\xi \lesssim 0.25$. During the early stage the evolution is damped, but at the time $t = 25$ the damping is turned off and then the field is allowed to evolve freely. Domains where ϕ is in either of the two minima of the potential (3) are formed and separated by domain walls. As is well-known the domains grow in size during the evolution; a numerical study of the scaling properties of domain walls in classical ϕ^4 theory is reported in [31] and very recently confirmed in the quantum theory in the semiclassical approximation in [32].

Obviously, a domain wall itself is an energy concentration due to the potential and gradient energy locked up in the wall, and a moving wall has naturally also a kinetic component. When a domain collapses the energy that was trapped in the domain wall is released. Thus there is energy available for the field to execute large oscillations. The simulations carried out here point out that usually the domain collapse takes place rapidly and then there tends to be large amount of energy, especially in the kinetic form, localized around the quickly shrinking domain wall already well before the eventual disappearance. In particular, there appear some very high energy concentrations moving along the wall. A similar kind of observation of energy concentrations, often (but not necessarily) along the domain wall, was made in [33] where field dynamics of tachyonic preheating after hybrid inflation was studied. Once the domain has collapsed these energy concentrations either give rise to or turn into propagating nonlinear waves. Oscillons are born.

The process of domain collapse is illustrated with two pairs of snapshots. Figure 4 shows the isocontours of the field ϕ (left) and the energy density (right) before (above) and after (below) the domain collapse. Inside the contours dark gray indicates a region where the field is close to the disappearing vacuum; in the areas in lighter gray the field is around the maximum of the potential, and white marks the field close to the other vacuum that becomes the dominating one. In turn, the higher the energy density, the darker the corresponding area is displayed, and the pentagonlike shape of the domain is also clearly recognizable in the corresponding snapshot of the energy density where the enclosing domain wall appears black. In the second pair of snapshots the domain has collapsed—the large gray area has vanished indicating disappearance of this vacuum. Instead there are ripples where the field is far from the dominating vacuum positioned on a ringlike wave front. These small, elliptic regions show up in extremely high peaks of energy density (the view in the picture is tilted to visualize the height of peaks of energy concentration). These are oscillons which propagate along the spherical wave front away from the location of the collapsed domain. Unlike the dispersive waves that are damped quickly, oscillons are far less dissipative and have a long range. It should be noted that the elliptic form results from Lorentz contraction and thus indicates the high velocity of emitted oscillons. Furthermore, the seeds of oscillons are not required to be spherical: asymmetric bubbles can collapse into an oscillon [34]. The production of oscillons is associated with regions of high velocity on the domain walls, rather than bubble collapse where a single oscillon is formed from a bubble: there are generally several oscillons created by one collapsing domain.

A. Statistical analysis in frequency space

Eventually one or the other of the two minima will completely dominate in a lattice of a finite size. However, if the simulation box becomes divided between two domains that span over the whole volume, typically a fairly static, intermediate state follows where there are

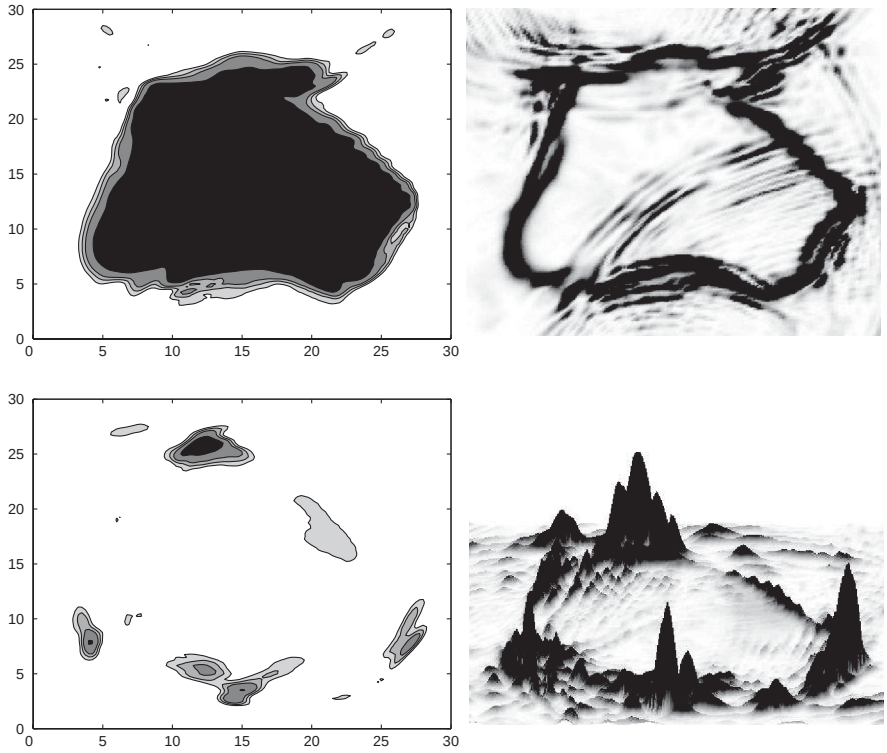

FIG. 4. Oscillon formation in a domain collapse: the left panel shows contours of the field ϕ; the right panel presents the total energy density before the domain collapse (above) and right after (below). The snapshots are separated by 27 time units; the physical size in linear dimension of the subbox shown is 30.

those two domains, and domain walls, present and which last for a long time. We exploit this phenomenon in order to compare the signal of oscillons and domain walls in the spectral function.

It is relatively easy to observe if there are only one or two large domains present by monitoring the total length of domain walls in the lattice. If the total length of domain walls does not exceed twice the linear size of the lattice L, there cannot be two domains spanning the box size. We determine the length of domain walls by counting the number of lattice sites where the field changes sign compared to its nearest neighboring lattice points. We work under the hypothesis that oscillons are created only when larger domains collapse, thus from the last domain of the disappearing vacuum and the ones from smaller domains created earlier disappear when colliding with the domain walls still present (though as demonstrated later on this is not inevitably the outcome).

We generated 30 000 different initial configurations. Since our attention is in the aftermath of collapsed domains, the simulations are evolved much longer than in a study interested in the scaling regime ($t \lesssim L/2$). We monitor the length of domain walls at two instants: $t = 250$ and $t = 750$. Out of all the configurations, in 18 931 there is only one large domain dominating at the time of the first inspection. In 8174 cases the simulation box was divided into two large domains throughout this interval up to the final time $t = 750$. In the remaining cases the collapse of the other domain takes place during this interval and these events are discarded here.

We examine the spectral function separately for these two above mentioned cases—single domain (oscillons) or two domains (and thus long domain walls present). Figure 5 shows the spectral function $|\rho(\omega)|$ obtained an average over all the selected configurations and normalized by the number of events for one domain present (black) and for two domains (gray). The Fourier transform is made over the time interval of the length 400 starting at time $t = 350$. This choice is to ensure that if there are shorter domain walls present at the time $t = 250$ that do not trigger the threshold $2L$ when monitoring is made, they have time to fade during the subsequent time interval before the observation interval commences.

For a single domain with oscillons the spectral function shows a fairly broad radiation peak, and a long ''shoulder'' of decreasing power together with almost complete absence of lowest frequencies. This is in stark contrast with the growing power at small frequencies in presence of two domains. We believe this is the signal of the long domain walls that are very static objects, thus contributing to the lowest frequencies in the system. The peak at the radiation frequency is also narrower. This is easily understood by the fact that there is less kinetic energy in the system as a large fraction of the energy remains locked up in the long

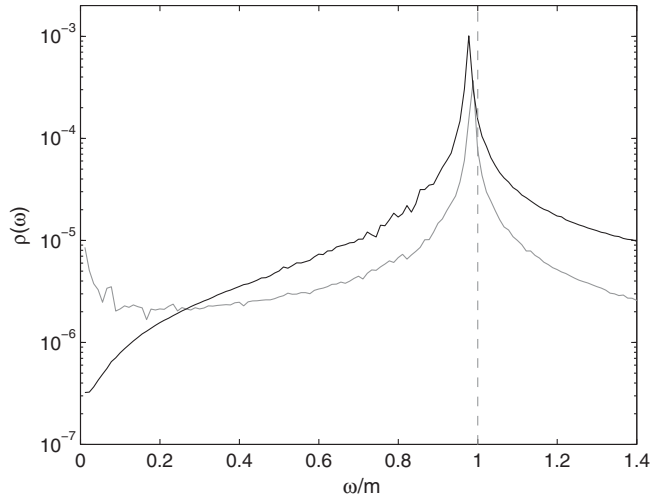

FIG. 5. The spectral function $|\rho(\omega)|$ at zero momentum over the time interval of length 400 for oscillons (black) and domain walls (gray). The vertical dashed line shows the radiation frequency $\omega = m$ without fluctuations.

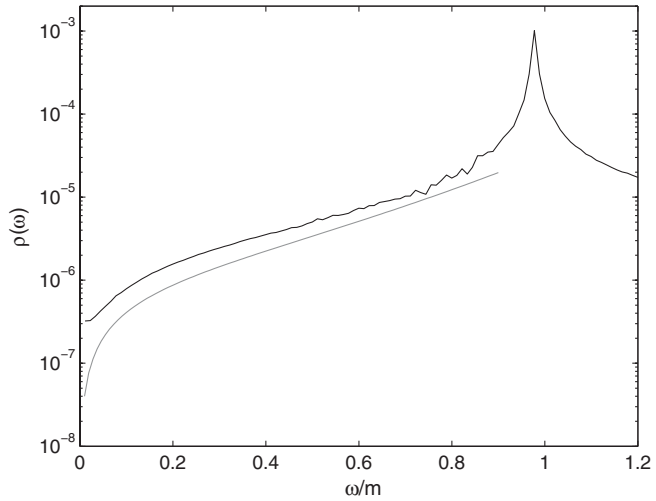

FIG. 6. The spectral function $|\rho(\omega)|$ for oscillons (black) as in Fig. 5 together with the curve $\omega \cdot \exp(b\omega^2)$ (gray), where $b = 2.1$.

domain walls. Thus these are cooler systems compared to those without domain walls. Not only the width, but also the location of the peak of radiation confirms this. In neither of the cases is the peak positioned precisely at $\omega = m$, but at a slightly lower frequency. This is because the effective mass in the theory is less than the bare parameter m due to the fluctuations of the field yielding a negative correction. In case of one domain the fluctuations are naturally larger and the shift is already visible effect yielding approximately 2% dislocation from $\omega = m$. We doubt that temperature could be derived via kinetic energy in these cases yielding a sensible result because of the presence of oscillons which carry considerable kinetic energy, but should not be considered as thermal fluctuations. Other numerical studies have estimated that a half [35] or even the majority [18] of the energy of a system could be stored in oscillons. Oscillons have been seen to act as a bottleneck of equipartition for modes corresponding large wavelengths and thus at the very least delaying system's approach to the equilibrium [36].

The time dilation of the oscillation period relates the frequency and velocity via $\omega = \omega_0/\gamma$ and it is thus appealing to try to extract information of the velocity of oscillons from the power in the spectral function assuming that the signal in spectral function at frequencies $\omega \lesssim 0.85$ is mainly due to the oscillons. Figure 6 shows that the shoulder can be reproduced. The signal in the spectral function $\rho(\omega)$ can be transferred to an arbitrary velocity distribution $n(v)$ with the use of the amplitude given by (A4). One now needs to assume that the formed oscillons have typical size $r_0 \approx 3$—this is supported by the simulations. Figure 7 shows the velocity distribution as a function of γ-factor derived by (A7) from the signal in spectral function. The data suggest fairly flat distribution at low velocities, whereas the region $\gamma \gtrsim 2$ is well fitted with a power law suppression γ^{-2}. It is an open question whether this velocity distribution reflects the properties of the source, or the effect of energy loss in the strongly radiative environment (oscillon survival in thermal environment has been studied in [37]). Conservation of momentum indicates that the high-γ oscillons must be emitted by high-γ parts of the domain wall network. These are cusps, which are by definition regions where the walls are moving close to the speed of light.

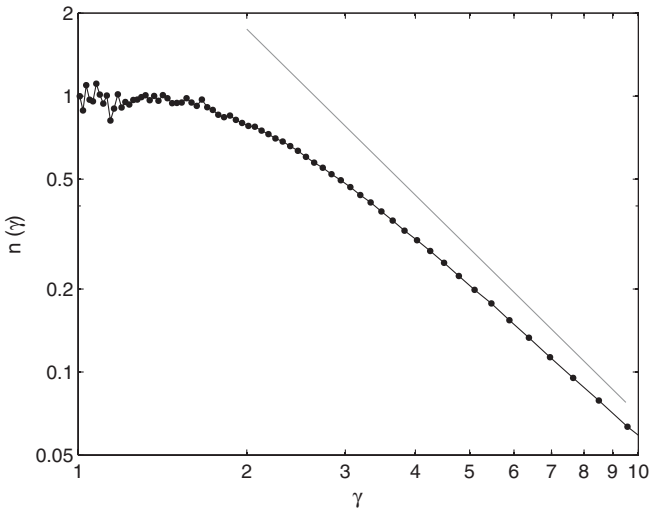

FIG. 7. The velocity distribution $n(\gamma)$ derived from the signal in spectral function $\rho(\omega)$. The distribution is normalized to unity at the data point of smallest velocity $v \simeq 0.12$. The parameters ω_0 and r_0 are set to have the same values as in Fig. 3. The straight, gray line is a guide to eye showing curve γ^{-2}.

V. OSCILLON GAS

While simulations with random initial conditions and the subsequent formation of oscillons from collapsing domains provide reasonably realistic model of how oscillons could be produced e.g. in conditions present in the early Universe, the drawback is the strong radiative component. Inevitably, a large fraction of the energy of the domain walls is released into dispersive modes that not only appear as the dominating signal in the spectral function, but also undoubtedly effect significantly the evolution of oscillons as discussed earlier.

In order to simulate the evolution of an ensemble of oscillons in a far less radiative environment, we followed a different approach. An *oscillon gas* is initialized by preparing an oscillon lattice where oscillons are placed initially at equal distance from each other, but boosted with a velocity v in random directions. In the subsequent evolution oscillons collide resulting in scattering, decaying, and merging. The energy released from oscillons creates a radiative component, but this is starkly suppressed compared to the one present in simulations reported in the previous section.

Figure 8 shows three snapshots of the total energy density in a simulation where initially 36 oscillons at velocity $v = 0.5$ into random directions are placed on the lattice of size 800^2 (physical size in linear dimension is 200). There is a reduction in the number of oscillons, and energy in dispersive propagating waves is clearly visible in the two later snapshots, but this is far less strong than those originating from domain walls. Most importantly, the simulations show that few oscillons, typically half a dozen, survive for a long period of time, far greater than e.g. the time required an oscillon at initial velocity v to travel around the lattice.

Because radiation is suppressed, higher concentrations in the energy density can be used to track oscillons. The survival of oscillons was studied more quantitatively by performing simulations of a larger ensemble. One hundred different initial states each having 121 oscillons at the beginning were evolved on a lattice of size 1500^2. Figure 9 shows the fraction of lattice points where the total energy exceeds 0.25, 0.2, or 0.15 as a function of time (these thresholds correspond roughly 35, 28, and 20 times the mean value, respectively). For clarity the data is averaged over one oscillation period (roughly 5 in time units). This is because all the oscillons start initially at the same phase and there is considerable variation in the height and width of the energy density within the period (see [38]). Some oscillations are still visible left in Fig. 10, where the same data is plotted on a logarithmic scale. All the curves yield similar time evolution; thus we conclude that there is no sensitivity to the thresholds chosen. As the dispersive waves do not contain such energy concentrations that would exceed these thresholds as can be seen in Fig. 8, we further argue that the signal must be due to oscillons.

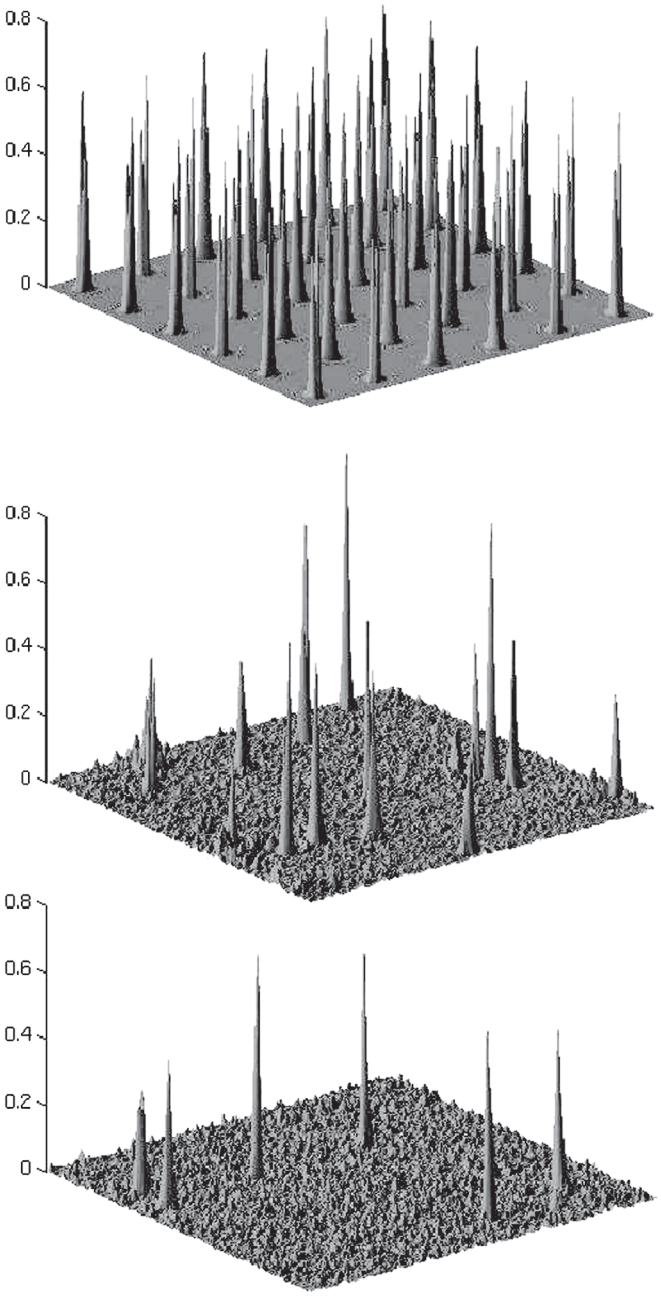

FIG. 8. Sequence of snapshots showing the total energy density at times $t = 0$, 937.5, 10190.

The data in Figs. 9 and 10 clearly show that there is a decrease in number of lattice sites where energy density exceeds the thresholds corresponding the demise of oscillons in collisions. However, the main result is that there are two phases: steeply declining slope flattens around time $t = 10^3$ to a much less rapid decay. At the end of the simulation there is still almost 20% left of the initial number of lattice points where the thresholds are exceeded.

In the region of fast decline the slopes have values approximately -0.7. This is marginally consistent with a decay law inversely proportional to time. Such a power law

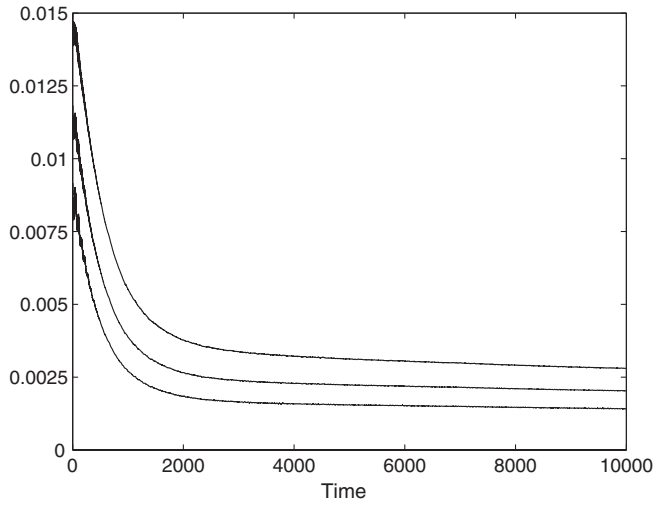

FIG. 9. Fraction of points of the lattice where the total energy density exceeds 0.15, 0.2, or 0.25 (20, 28, and 35 times the average from top to bottom) as a function of time.

is to be predicted by a simple annihilation picture: oscillons have constant velocity v and cross section σ. Then in two dimensions their number density $N = N(t)$ obeys the differential equation

$$\dot{N} = -\langle v\sigma\rangle N^2, \tag{9}$$

which yields evolution inversely proportional to time, or more precisely

$$N(t) = \frac{N_0}{1 + \langle v\sigma\rangle N_0 t}. \tag{10}$$

While the steeper slopes can be understood on the basis of the differential equation (9), we do not have any quantitative explanation for the crossover. On the qualitative level there are at least two effects that could lengthen the life time of oscillons at a later stage of the simulations. First, collisions between oscillons, though not necessarily leading to a demise, cause considerable perturbation, and the oscillon radiates strongly before it settles back into a long-living state. If another collision occurs during this relaxation stage that is then presumably highly likely to destroy the already perturbed oscillon. In the simulations it is seen that the second collision is indeed often the fateful one. Lower number density and consequently a longer mean free path can yield an enhancement of the survival probability in collisions. More importantly, due to the interactions oscillons slow down drastically (a decrease in the average velocity $\langle v\rangle$ can be partially responsible of the flatter slope than the expected -1 at the earlier stage). The reduced collision rate in turn increases the lifetime.

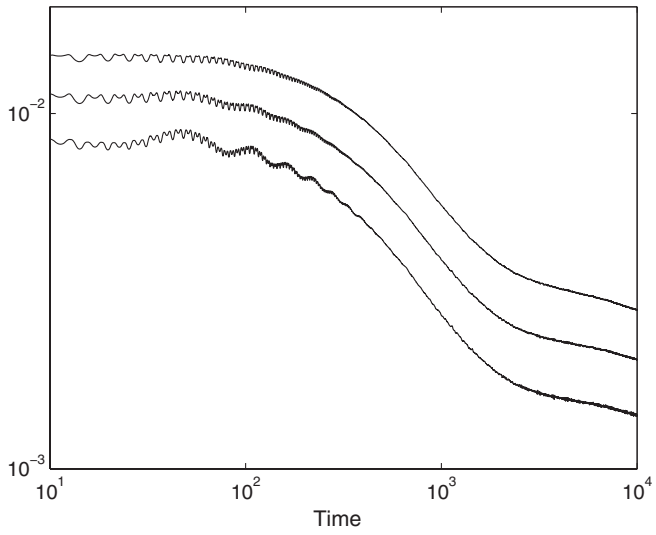

FIG. 10. The same data as in Fig. 9 on a logarithmic scale.

VI. OSCILLON COLLISIONS—MERGING AND SCATTERING

The simulations presented in previous section show that collisions between oscillons can, apart from scattering or demise, result to merging. Off-axis collisions of oscillons were briefly studied in [38] reporting an attractive scattering. A wider study at lower velocities were performed here. Reducing the velocity causes the trajectories of oscillons to bend more after the encounter. Ultimately oscillons scatter approximately at right angles after the collision. Below this critical velocity the oscillons do not scatter anymore, but merge together. This is illustrated in Figs. 11 and 12. Figure 11 shows snapshots of the value of the field in an off-axis collision of two oscillons when the displacement in the alignment between the centers of oscillons, the impact parameter, is 11.0 units. On the left panel the initial velocity is set to be $v \simeq 0.1$ whereas on the right it is approximately 10% smaller, $v \simeq 0.09$. In the previous case scattering takes place, including a strong phase shift. The latter situation results to merging where a considerable amount of energy is leaked during the process as can be seen from the spiral waves in the field. However, a localized energy concentration remains as can be seen particularly clearly in Fig. 12, which shows the energy density at same time instants as the value of the field in Fig. 11.

Impact parameter alone, however, is not sufficient for a complete description of the scattering process of oscillons. As mentioned before, over a period of an oscillation there is a large variation in the size of the concentration an oscillon causes in energy density. Therefore the bare impact parameter is an inadequate simplification, but also the phase at the moment of the impact affects the energy transfer and thus the final state after the collision. An exhaustive study of these effects was not carried out here. We merely finish by reporting that at low velocities even an impact parameter as large as 12 in the units used, thus greatly exceeding the approximate size of an oscillon r_0, is still sufficient to bend the trajectories to such an

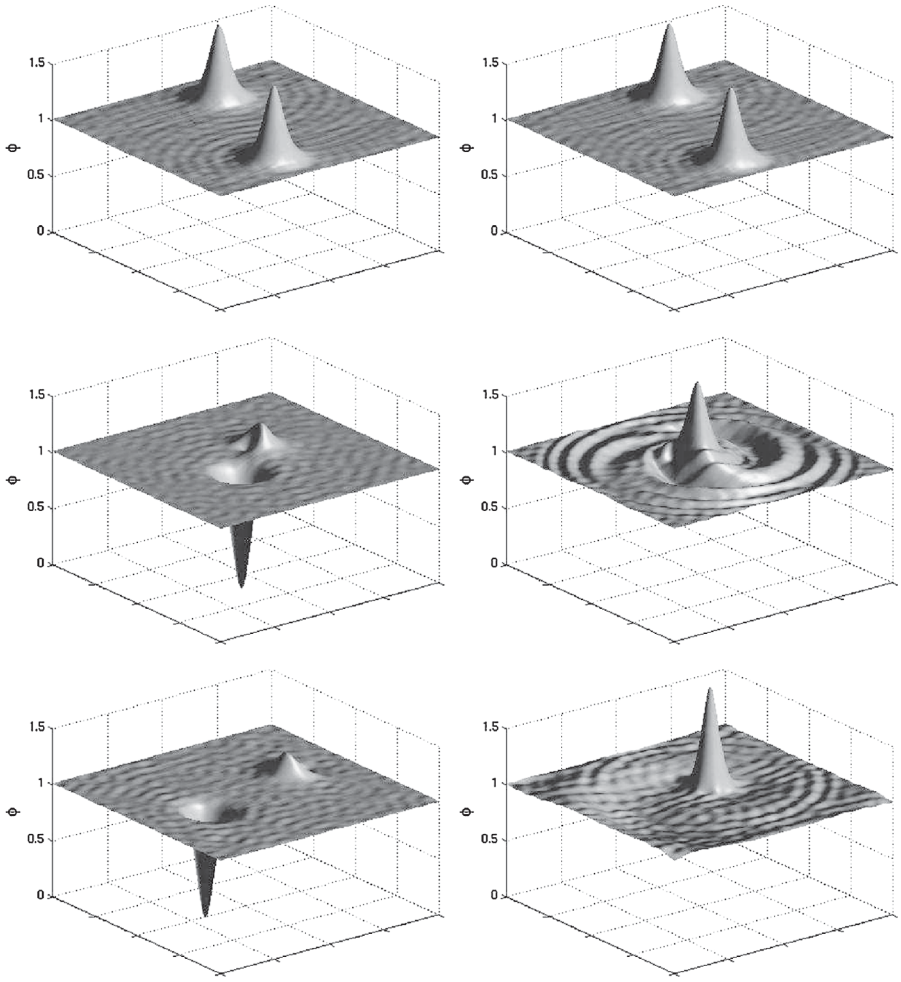

FIG. 11. Oscillons scattering and merging: the field at three instants (chronologically from top to bottom) in an off-axis collision of oscillons at velocity $v \simeq 0.1$ (left) and $v \simeq 0.09$ (right). Alignment of the centers is displaced by 11.0 units.

extent that oscillons merge together. None of the setups used for collisions have led to an immediate demise of both oscillons, but the final state has always at least one localized energy concentration left.

VII. OSCILLONS CROSSING THE DOMAIN WALLS

As oscillons are made by domain walls and survive collisions, it is natural to pose the question what happens when an oscillon meets a domain wall. Figure 13 shows snapshots of an oscillon with an initial velocity $v \simeq 0.75$ crossing a domain wall. The oscillon is clearly recognizable both before the encounter and afterwards oscillating around the other vacuum. Snapshots of the total energy density show that crossing has caused a perturbation on the domain wall that propagates at the speed of light along the wall away from the interaction point. Snapshots in the kinetic energy where the static domain wall is initially invisible show that while the oscillon has shed some energy to the domain wall, that is a relatively tiny fraction as the ripples along the domain wall are barely visible. Though the direct energy transfer between the oscillon and the domain wall is in this case relatively small, the oscillon is deformed, slightly elongated in the direction of the domain wall, and potentially radiates some of its energy. It should be emphasized that the presented encounter is not necessarily a typical one—at velocity $v \simeq 0.5$ a crossing and survival, large localized oscillations has not been witnessed. At $v \simeq 0.5$ energy density of an oscillon does not greatly exceed that of a domain wall, whereas at $v \gtrsim 0.75$ it is factors larger. In addition, there are two effects that readily seem to enhance the crossing probability at higher velocities. Lorentz contraction shortens the length of the disturbance oscillons create and the lower frequency and thus slower time evolution of the wave decreases the energy transfer to the domain wall. Apart from the velocity, the relative phase of the oscillon seems to strongly control the amount of energy transfer in a collision. In any case, just the potential of oscillons crossing domain walls and propagate from one vacuum to another demonstrates how surprisingly persistent objects they are.

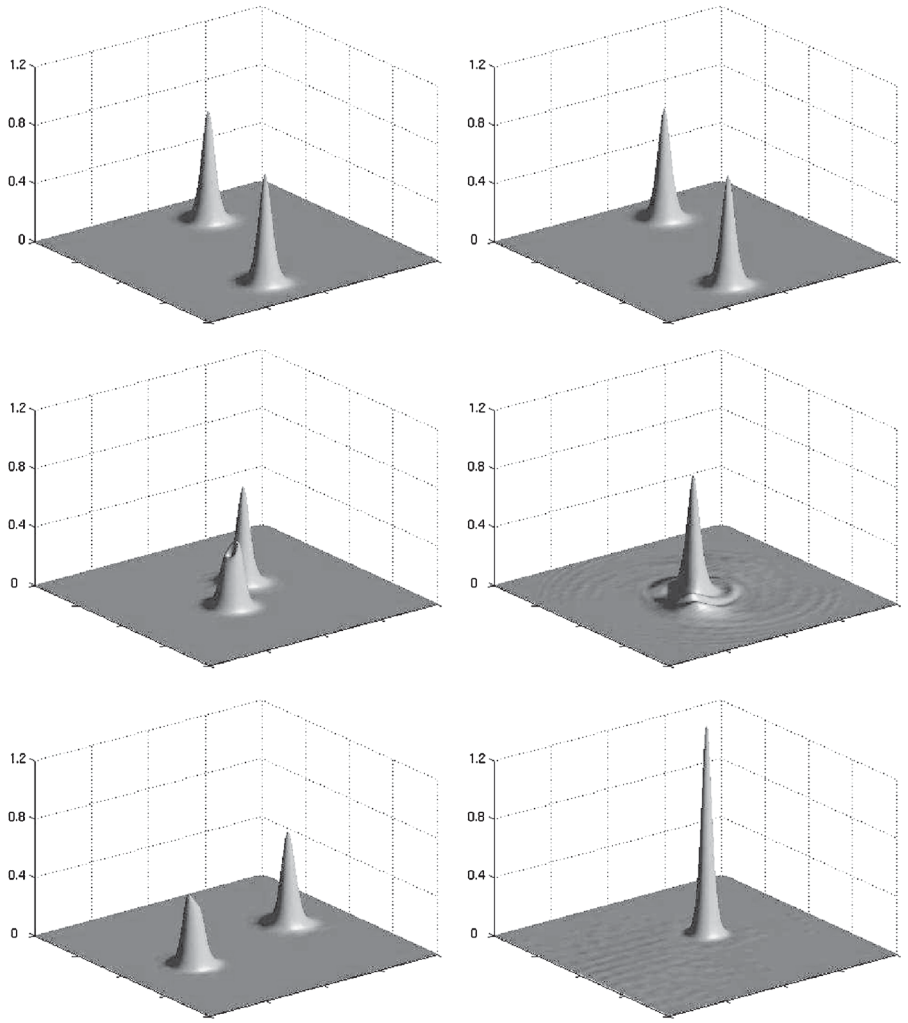

FIG. 12. Oscillons scattering and merging: the energy density at the same time instants as in Fig. 11 in an off-axis collision of oscillons at velocity $v \simeq 0.1$ (left) and $v \simeq 0.09$ (right).

VIII. CONCLUSIONS

We have studied the field dynamics of a quartic double-well potential with random initial conditions in two spatial dimensions. We have shown evidence that when the field is undamped the collapse of domains takes place so rapidly that there is enough energy to excite the field into long-lived, nonperturbative oscillating energy concentrations, or oscillons. Investigating the field in the Fourier domain using a kind of classical spectral function enabled us to extract a velocity distribution for the oscillons, which extends to surprisingly high γ, which we believe originate from regions from the domain wall with high velocity or cusps. We note that long domain walls also leave a very distinctive trace in the spectral function and maybe similar techniques could be used in studies of defects as well.

We further examined oscillons in a less radiative environment but in still a random system and shown that a fraction of oscillons persist for a long time. We reported on merging of oscillons in off-axis collisions at low velocities as well as the potential of oscillons to cross a domain wall at high enough velocity. We believe these results would be qualitatively very similar in the two-dimensional sine-Gordon model that supports oscillons as well. Extrapolation to three dimensions, however, is far less straightforward as the lifetime and stability of oscillons depends strongly on the dimension of the theory. Adequate simulations would be required there.

We did not impose any damping for the system apart from at very early times to condense it. Damping is not likely to alter the process of domain collapse considerably, unless the dissipation is really strong, while the further evolution may be different. However, it is not clear what kind of consequences dissipation would have. Damping could reduce the dispersive radiation modes and thus even enhance the oscillon lifetime. An obvious reason for friction in the system is the Hubble damping in the early Universe. A numerical study in one dimension showed that oscillons could persist in an expanding background when the expansion rate is low enough [39]. This has been

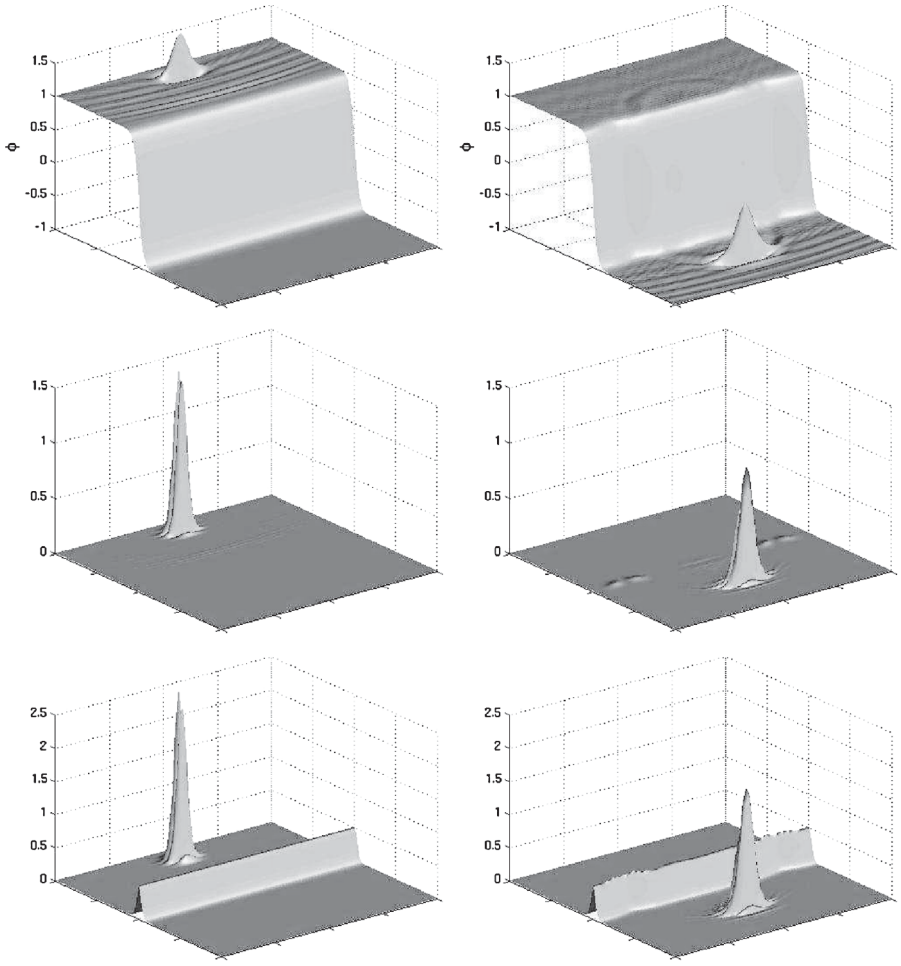

FIG. 13. An oscillon crossing a domain wall: the upper panel shows the value of field before (left) and after (right) the collision; the middle shows the kinetic energy density and total energy below.

recently studied analytically and the rate of energy loss was shown to be exponentially suppressed in the inverse of the Hubble parameter H [35]. Going back to moving oscillons and their interactions, expansion can reduce velocities which may once again have twofold consequences, oscillons may merge and demise in collision easier, but may also reduce collision rate and then increase the lifetime.

ACKNOWLEDGMENTS

We thank Gert Aarts, Szabolcs Borsanyi, Ajit Srivastava, Anders Tranberg, and Tanmay Vachaspati for discussions. P. S. was supported by the Netherlands Organization for Scientific Research (N.W.O.) under the VICI programme. This work was in part initiated when P. S. was supported by Marie Curie Fellowship of the European Community Program Human Potential under Contract No. HPMT-CT-2000-00096.

APPENDIX A

We present here an analytic outline how moving Gaussian distribution would appear in spectral function $\rho(\omega)$. The starting point is the ansätze (7) and (8). Assume now further that all the modes $f_n(r)$ have the Gaussian form with the same width

$$\phi(r, t) = \exp(-r^2/r_0^2) \cdot \sum_{n=1}^{\infty} a_n \cos(n\omega_0 t). \tag{A1}$$

Consider now an arbitrary term in the sum under a boost with velocity v in x_1-direction. This yields

$$a_n \exp\left(-\frac{\gamma^2 u^2 + x_2^2}{r_0^2}\right) \cdot \cos\left(n\omega_0\left(\frac{t}{\gamma} - \gamma v u\right)\right), \tag{A2}$$

where we have defined $u = x_1 - vt$. The volume average integrating over the variables u and x_2 yields

$$\frac{a_n}{\gamma} \exp\left(-\frac{n^2\omega_0^2 r_0^2}{4} v^2\right) \cdot \cos\left(\frac{n\omega_0 t}{\gamma}\right). \tag{A3}$$

The decrease in the frequency is now explicitly readable in the time-dependent part. Turning to the basic frequency, set $n = 1$ (it is also noticeable that the higher modes $n > 1$ that appear with weaker amplitudes a_n undergo an extra suppression, which is to a certain extent visible in Fig. 1,

compared to the static situation $v = 0$). Spectral function in the approximation used is the product $\bar{\Pi} \cdot \bar{\phi}$. Thus its amplitude has functional dependence on the kinematic variables v and γ

$$A(v) \propto \frac{1}{\gamma^3} \exp\left(-\frac{1}{2}\omega_0^2 r_0^2 v^2\right). \tag{A4}$$

Consider now an arbitrary velocity distribution $n(v)$. This yields a signal in spectral function

$$\rho(\omega) \propto \int dv n(v) A(v) \delta(\omega - \omega_0/\gamma(v)). \tag{A5}$$

By the simple relation $\gamma = \omega_0/\omega$ this can be turned to the velocity distribution

$$n(v) = \frac{\omega_0\sqrt{\omega_0^2 - \omega^2}}{\omega} \frac{\rho(\omega)}{A(\omega)}. \tag{A6}$$

It is, however, better suited to present the distribution n as a function of γ-factor

$$n(\gamma) = n(v) v/\gamma^3. \tag{A7}$$

[1] T. W. B. Kibble, J. Phys. A **9**, 1387 (1976).
[2] W. H. Zurek, Nature (London) **317**, 505 (1985).
[3] M. Hindmarsh and A. Rajantie, Phys. Rev. Lett. **85**, 4660 (2000).
[4] S. R. Coleman, Nucl. Phys. **B262**, 263 (1985).
[5] I. L. Bogolyubsky and V. G. Makhankov, JETP Lett. **24**, 12 (1976).
[6] I. L. Bogolyubsky and V. G. Makhankov, Pis'ma Zh. Eksp. Teor. Fiz. **25**, 120 (1977).
[7] M. Gleiser, Phys. Rev. D **49**, 2978 (1994).
[8] E. J. Copeland, M. Gleiser, and H. R. Muller, Phys. Rev. D **52**, 1920 (1995).
[9] E. Farhi, N. Graham, V. Khemani, R. Markov, and R. Rosales, Phys. Rev. D **72**, 101701(R) (2005).
[10] N. Graham, Phys. Rev. Lett. **98**, 101801 (2007).
[11] N. Graham, Phys. Rev. D **76**, 085017 (2007).
[12] M. Dine and A. Kusenko, Rev. Mod. Phys. **76**, 1 (2004).
[13] A. Riotto, Phys. Lett. B **365**, 64 (1996).
[14] G. Fodor, P. Forgacs, P. Grandclement, and I. Racz, Phys. Rev. D **74**, 124003 (2006).
[15] P. M. Saffin and A. Tranberg, J. High Energy Phys. 01 (2007) 030.
[16] H. Arodz, P. Klimas, and T. Tyranowski, Phys. Rev. D **77**, 047701 (2008).
[17] M. Gleiser, Phys. Lett. B **600**, 126 (2004).
[18] M. Broadhead and J. McDonald, Phys. Rev. D **72**, 043519 (2005).
[19] M. van der Meulen, D. Sexty, J. Smit, and A. Tranberg, J. High Energy Phys. 02 (2006) 029.
[20] E. W. Kolb and I. I. Tkachev, Phys. Rev. D **49**, 5040 (1994).
[21] B. Piette and W. J. Zakrzewski, Nonlinearity **11**, 1103 (1998).
[22] S. Kasuya, M. Kawasaki, and F. Takahashi, Phys. Lett. B **559**, 99 (2003).
[23] M. Onorato, A. R. Osborne, M. Serio, and S. Bertone, Phys. Rev. Lett. **86**, 5831 (2001).
[24] M. Gleiser and J. Thorarinson, Phys. Rev. D **76**, 041701 (R) (2007).
[25] M. Gleiser, B. Rogers, and J. Thorarinson, Phys. Rev. D **77**, 023513 (2008).
[26] I. Dymnikova, L. Koziel, M. Khlopov, and S. Rubin, Gravitation Cosmol. **6**, 311 (2000).
[27] G. Aarts and J. Smit, Nucl. Phys. **B511**, 451 (1998).
[28] G. Aarts, Phys. Lett. B **518**, 315 (2001).
[29] R. Watkins, Report No. DART-HEP-96/03, 1996 (unpublished).
[30] E. P. Honda and M. W. Choptuik, Phys. Rev. D **65**, 084037 (2002).
[31] T. Garagounis and M. Hindmarsh, Phys. Rev. D **68**, 103506 (2003).
[32] S. Borsanyi and M. Hindmarsh, Phys. Rev. D **77**, 045022 (2008).
[33] E. J. Copeland, S. Pascoli, and A. Rajantie, Phys. Rev. D **65**, 103517 (2002).
[34] A. B. Adib, M. Gleiser, and C. A. S. Almeida, Phys. Rev. D **66**, 085011 (2002).
[35] E. Farhi *et al.*, Phys. Rev. D **77**, 085019 (2008).
[36] M. Gleiser and R. C. Howell, Phys. Rev. E **68**, 065203 (2003).
[37] M. Gleiser and R. M. Haas, Phys. Rev. D **54**, 1626 (1996).
[38] M. Hindmarsh and P. Salmi, Phys. Rev. D **74**, 105005 (2006).
[39] N. Graham and N. Stamatopoulos, Phys. Lett. B **639**, 541 (2006).